A two-component reflection seismic survey, Springbank, Alberta

Don C. Lawton and Mark P. Harrison

ABSTRACT

A converted-wave (P-SV) reflection seismic survey was recorded in conjunction with a conventional (P-P) survey over the eastern flank of the triangle zone near Springbank in the Rocky Mountain foothills. The processed radial-component section contains reflections from as deep as the PreCambrian basement, as well as from very shallow reflectors in Tertiary rocks. The vertical component data show clearly the eastern limit of deformation in the triangle zone, and the section obtained from data recorded with the vertical-component of single, 3-component geophones is comparable to that obtained from data collected using conventional geophone arrays.

Static corrections for the radial-component data set are uncorrelated with those for the vertical-component data set and residual shear-wave statics of up to 90 ms were calculated during the processing of the radial-component data. Reflections in the radial-component sections were enhanced considerably by the application of post-stack f-x and f-k filters.

INTRODUCTION

In recent years, there has been increasing interest in the acquisition, processing and interpretation of multicomponent seismic data for providing an improved image of the subsurface. Most previous studies in Alberta have been in the Plains, where most reflectors are flat-lying and hydrocarbon traps of interest are stratigraphic (Garotta, et al., 1985; Harrison, 1989).

Over the past 6 years, the Geophysics Field School at the University of Calgary has been acquiring conventional P-wave reflection data over the triangle zone in the Rocky Mountain Foothills west of Calgary. As part of the 1990 Field School, a 2-component reflection seismic program was undertaken to assess converted-wave (P-SV) surveys in areas of mild structure.

The term 'triangle zone' was introduced by Gordy et al. (1977) to describe structures found along the eastern margin of the Rocky Mountain thrust and fold belt. Eastward-dipping Upper Cretaceous and Tertiary strata are juxtaposed against westward-dipping, thrusted rocks of Paleozoic to Tertiary age, forming two sides of a triangle. Autochthonous rocks at depth form the base of the structure. Triangle zones in the Rocky Mountain Foothills have since been discussed by Price (1986), Jones (1982), Teal (1983), Charlesworth, et al. (1987), and McMechan (1985).

The triangle zone developed as the result of the displacement of a wedge of sedimentary rocks into the foreland basin. The wedge is bounded by roof and sole thrust

faults which Jones (1982) defined as the upper and lower detachments, respectively. The vergence of the sole thrust is foreland-directed, whereas that of the roof thrust is hinterland-directed. Tectonic delamination of the foreland succession occurs as the wedge is driven further into the basin. Sequences above the roof thrust are essentially autochthonous, except that they became uplifted as the wedging progressed.

Important gas fields occur in the western limb of the triangle zone (e.g. Turner Valley, Jumping Pound, Wildcat Hills), the reservoirs being located in carbonate rocks of Mississippian age in the hanging walls of major thrust faults. However, structural traps also occur in younger, Mesozoic rocks, such as in the Bearberry-Ricinus Cardium and Viking oil and gas field (Jones, 1989).

STUDY AREA

The 1990 University of Calgary Geophysics Field School seismic program was located at Springbank (Twp 25, Rge 4 W5), shown in Figure 1. Seismic data were collected along line FS90-1, which is located on the eastern flank of the Triangle zone near the Jumping Pound gas field. Line FS90-1 is 3 km in length and overlaps an older east-west industry seismic line which had been donated to the University (Figure 1).

An interpretation of the eastern portion of the industry seismic line is shown in Figure 3, with reflections correlated with geological markers from the stratigraphic column in Figure 2. This interpretation shows clearly the major thrust faults which form the upper and lower detachments of the triangle zone, and eastward-dipping reflections from rocks of the Edmonton (Upper Cretaceous) and Paskapoo (Lower Tertiary) Formations which lie above the upper detachment. Also of interest in the interpretation is another thrust fault (TF) which displaces the lower detachment and Upper Cretaceous markers, and appears to sole out within shales of the Blackstone Formation. A clear duplication of the Cardium Formation is evident.

The objectives of the Field School program were to extend seismic coverage further east of the industry line and to elucidate the eastward continuation of triangle zone deformation. Of particular interest was to test the applicability of a converted-wave (P-SV) survey in an area with mild structure and gently dipping reflectors. These objectives were met by recording a conventional P-wave survey as well as a 2-component (radial and vertical) survey along Line FS90-1.

DATA ACQUISITION

All data were acquired using seismic equipment owned and operated by the Department of Geology and Geophysics, University of Calgary. The conventional P-wave survey was recorded with 48-channel DFS-III instruments, and the 2-component survey was recorded with 96-channel Sercel 338HR instruments arranged in a 2x48 trace configuration. Hence, three separate 48-trace spreads were collected for each shot. Two-component recording was favoured over 3-component recording because of the limited number of channels available and the desire to have at least 48 channels of radial component data.

The instruments were slaved together and the common source consisted of 1 kg of dynamite loaded to a depth of between 10 and 15 m. This depth was chosen so that the

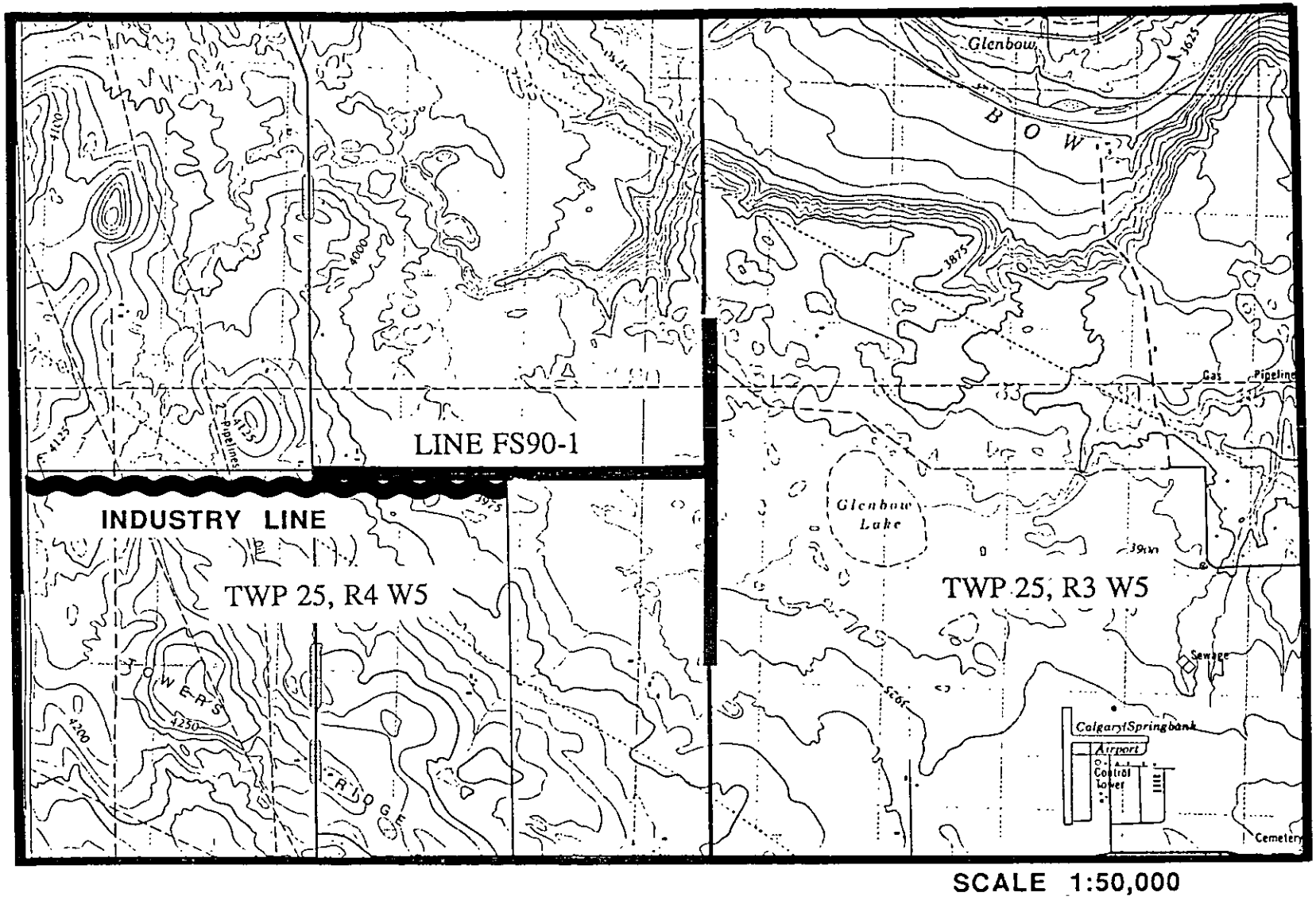

Fig. 1. Location map of Springbank area showing line FS90-1 and portion of existing industry line.

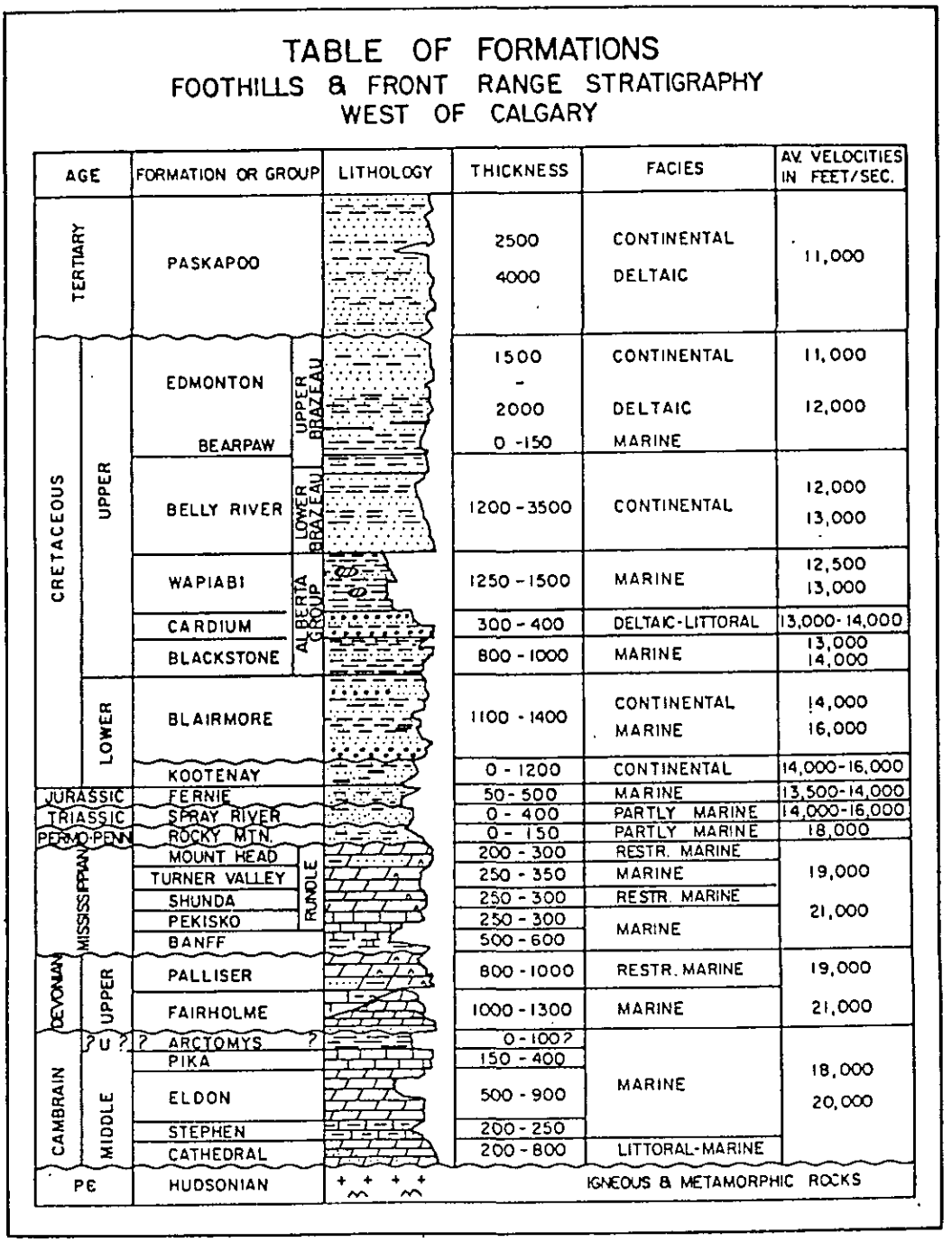

Fig. 2. Table of formations in the Foothills area west of Calgary (from CSPG Guidebook, 1975).

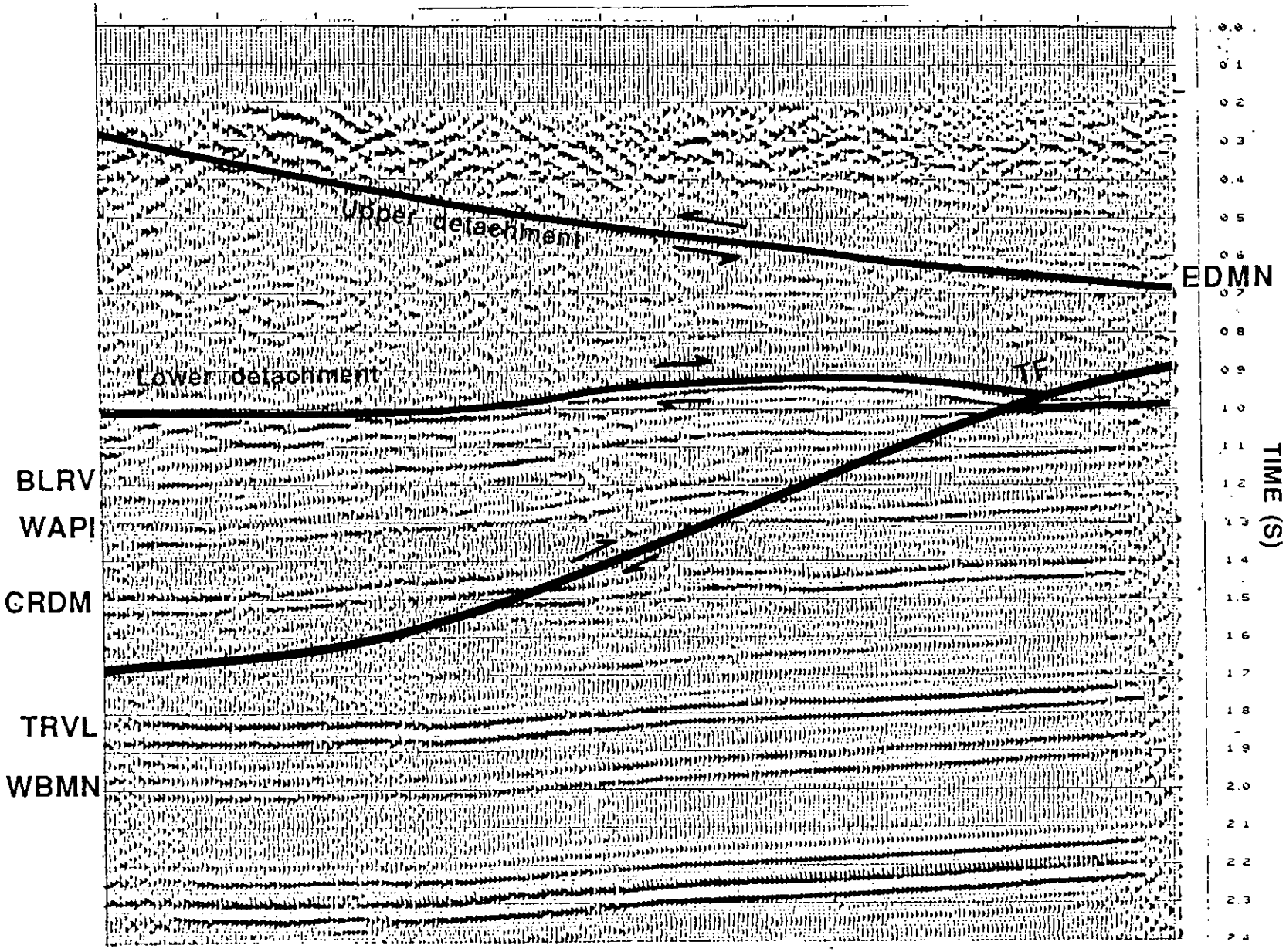

Fig. 3. Seismic section from east Jumping Pound.

dynamite was placed within a heavy clay layer, as this has been found to provide the most effective shot coupling. This clay layer is underlain by loose gravels which couple the shot energy poorly and are also difficult to drill through.

Table 1 shows the acquisition parameters used in the survey. The geometry used was similar to that from previous Field School surveys (Slotboom, et al, 1990) and is designed to provide optimum imaging of reflections in the first second of data. It was decided to use the same geometry for the 2-component survey as used for the conventional survey since modelling prior to the program showed that the amplitude of converted shear waves on the radial channel should be of the same order as the amplitude of compressional waves on the vertical channel for most offsets except the nearest traces. Synthetic P-P and P-SV shot gathers from the study area are shown in Figure 4. Thicknesses and P-wave velocities of the various geological formations were derived from Figure 2, and a constant Poisson's Ratio of 0.25 was assumed for the entire model (Poisson solid).

A near offset of only 30 m was retained in order to image the shallowest reflections possible for both P and S data. The nominal subsurface coverage was 24-fold, but the actual fold varied considerably because of the shortness of the line and the presence of a 400 m shot gap due to the proximity of a water well close to the line. For the conventional survey, recorded with the DFS III instruments, a low-cut filter of 12 Hz with a slope of 36 dB/octave was employed as this had been used sucessfully in past surveys in the area (after considerable testing). The choice of low-cut filters in the Sercel instruments was debated after some test records had been acquired. It was preferred initially that no low-cut filter should be used, but the high amplitudes of surface waves and multiple shear-wave refractions on the radial channel was of concern in terms of available dynamic range of the instruments. The only filter available with the instruments at the time of the survey was a 20 Hz low-cut filter but with a gentle slope of only 12 dB/octave. This filter was used, albeit with considerable reluctance. Examples of shot gathers from SP 161 are shown in Figure 5.

Table 1. Field acquisition parameters

Parameter	Conventional	2-component
Group interval	30 m	30 m
Shot size (common)	1 kg	
Shot depth	10-15 m	
Spread (end-on)	SP-30-1440 m, shot at west end.	
Geophones	M.P., 14 Hz	3-C Oyo, 10 Hz
Array	9 over 30 m	single
Instruments	DFS-III	Sercel 338HR
Channels	48	96
Low-cut filters	12/36	20/12
Notch (60 Hz)	in	in
Sample interval	2 ms	2 ms
Record length	4 s	6 s

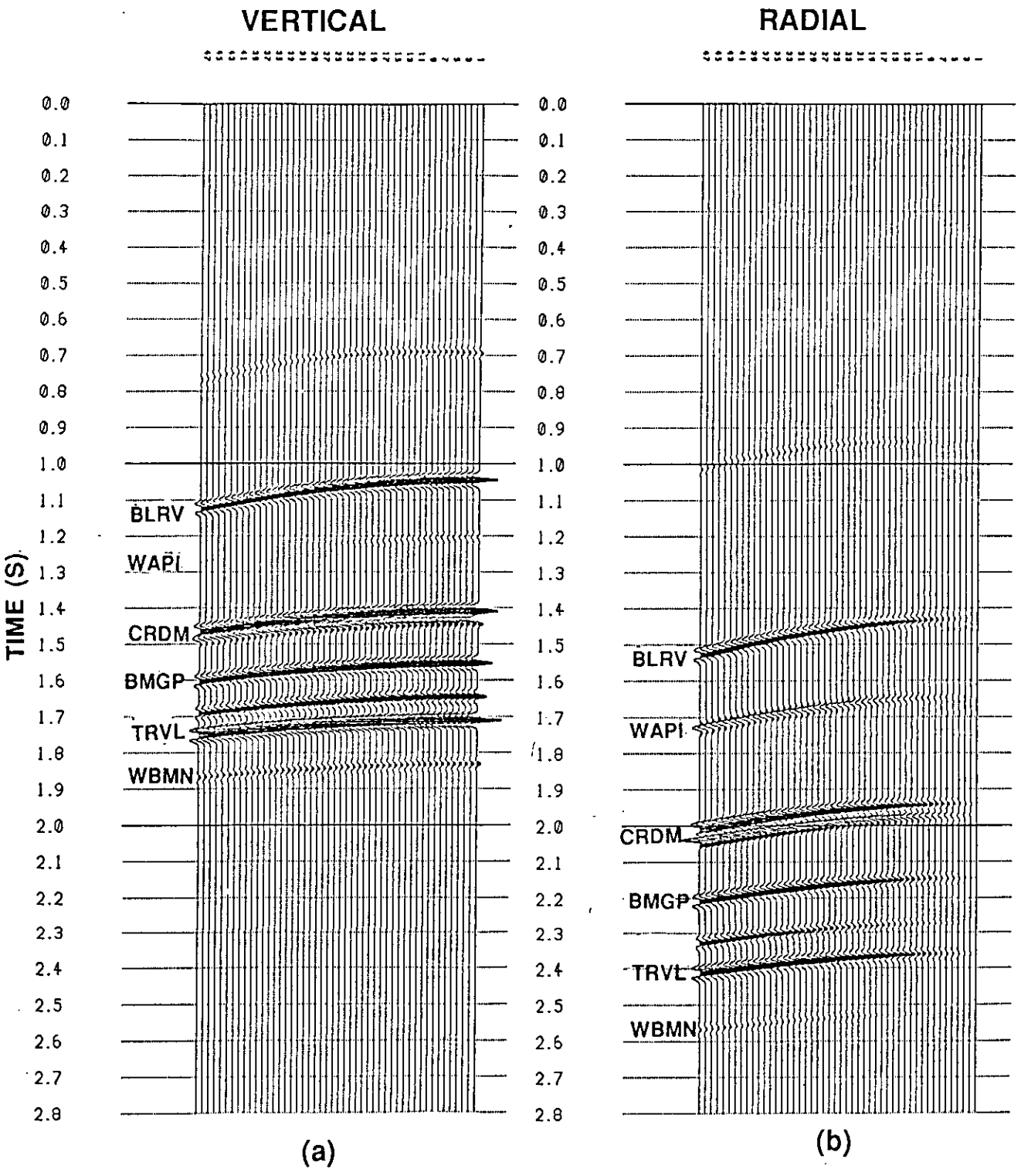

Fig. 4. Synthetic shot gathers with the same spread geometry used for the Field School program: (a) P-P; (b) P-SV.

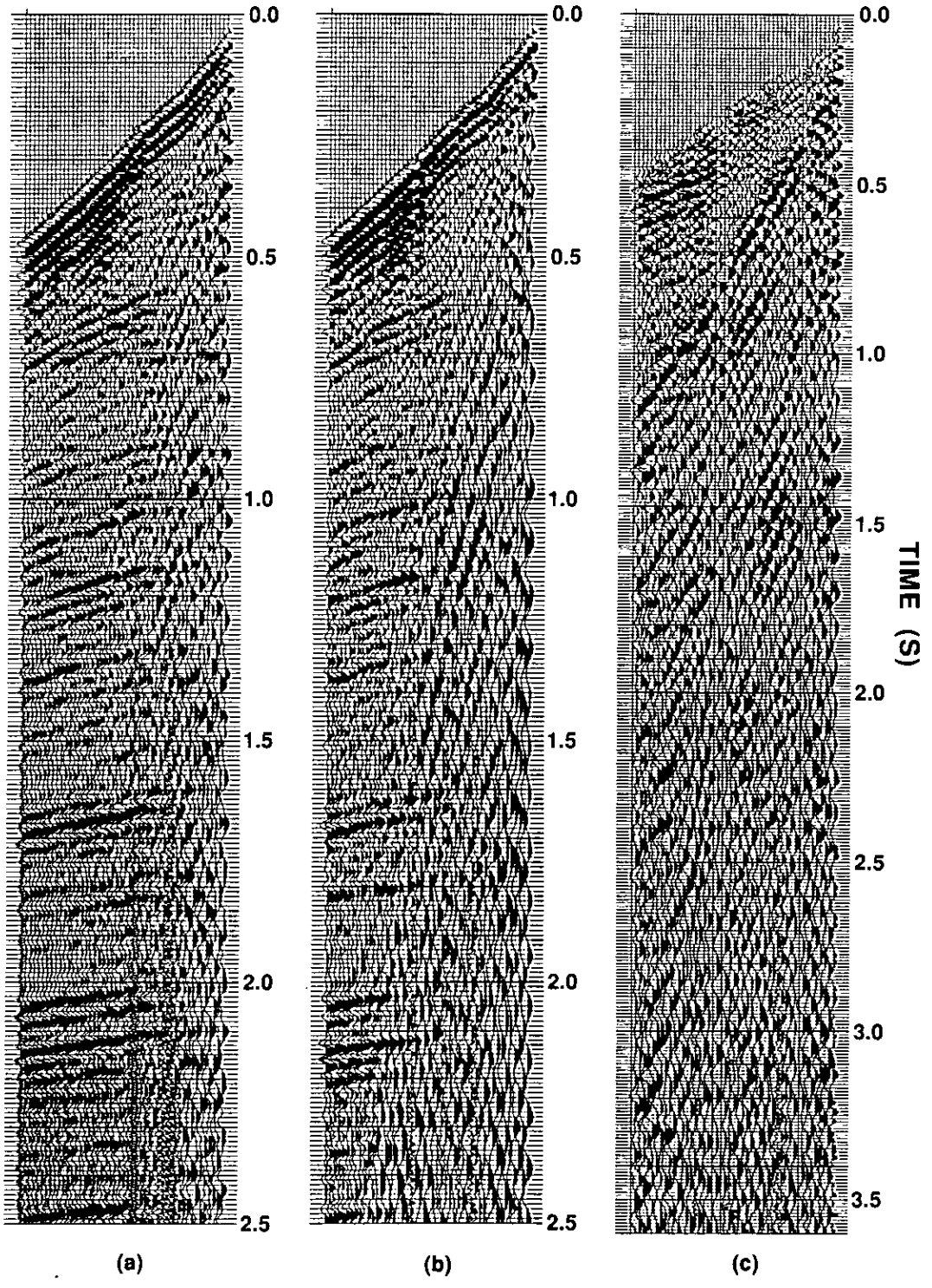

Fig. 5. Shot gathers from SP 161 of FS90-1: (a) conventional; (b) vertical component; (c) radial component.

DATA PROCESSING

The vertical (P-P) component of the two-component data set was processed using the flow shown in Figure 6. A double-gated spiking deconvolution was applied, due to the length of the data window. The initial elevation and refraction statics solution produced a gradual drop of about 16 ms in the structure times of the deeper events on the west end of the line. This drop was attributed to poor static control, and was removed using common source and common receiver stacks. The final stack section obtained is shown in Figure 7. To improve the signal-to-noise ratio, mainly in the shallow part of the section, an f-x prediction filter was applied to the unfiltered stack, followed by a mild f-k filter, bandpass filter, and gain. The resulting section is displayed in Figure 8. Prediction operators seven points in length, designed on windows 500 ms long and 50 traces wide, were used in the f-x filtering process. The f-k filter was designed to attenuate data outside of ±4 ms of dip by 6 db.

The conventional data set was processed using the same deconvolution parameters, static solution and velocity functions as were used on the vertical component data. The resulting section is shown in Figure 9. To facilitate comparison with the vertical-component section, f-x and f-k filters were also applied post-stack (Figure 10).

The radial (P-SV) component data set was processed using the flow shown in Figure 11. Double-gated deconvolution was also applied to the P-SV data. The final statics solution from the vertical component data set was applied to the radial component. This static solution was found to be appropriate for the source component of the statics solution, but residual receiver statics as large as 90 ms were obtained using common-receiver stacks. For this data set, there is no apparent correlation between the P-P and P-SV static solutions, as can be seen from Figure 12. Estimates of the Vp/Vs ratios across various intervals were calculated by first correlating events between the P-P and P-SV stack sections to get interval transit times, then using the following formula;

$$V_p/V_s = \frac{2I_s}{I_p} - 1$$

where I_p is the P-P time interval, and I_s is the P-SV time interval. The radial component data was then stacked using both the asymptotic approximation (Fromm et al, 1985), with a Vp/Vs ratio of 2.08, and a more exact binning method, in which a time-variant Vp/Vs ratio is used (Eaton and Stewart, 1989). The stacks obtained using these two binning methods are shown in Figures 13 and 14 respectively. To improve the stack sections, an f-x filter, followed by an f-k filter, were also applied to these two setions, giving the sections shown in Figures 15 and 16. The parameters using in applying the f-x filter were identical to those used on the P-P sections. The f-k filter in this case was designed to attenuate data outside of ±4 ms of dip by 9 db.

DISCUSSION

The bandpass-filtered sections of the vertical-component data (Figure 7) and the conventional data (Figure 9) are quite similar, although the latter section contains slightly less random noise. Also of interest is the fact that the shallow data are better imaged on the conventional section than on the single-component section. It is usually expected that geophone arrays will smear shallow reflections and result in poorer stacked data than that

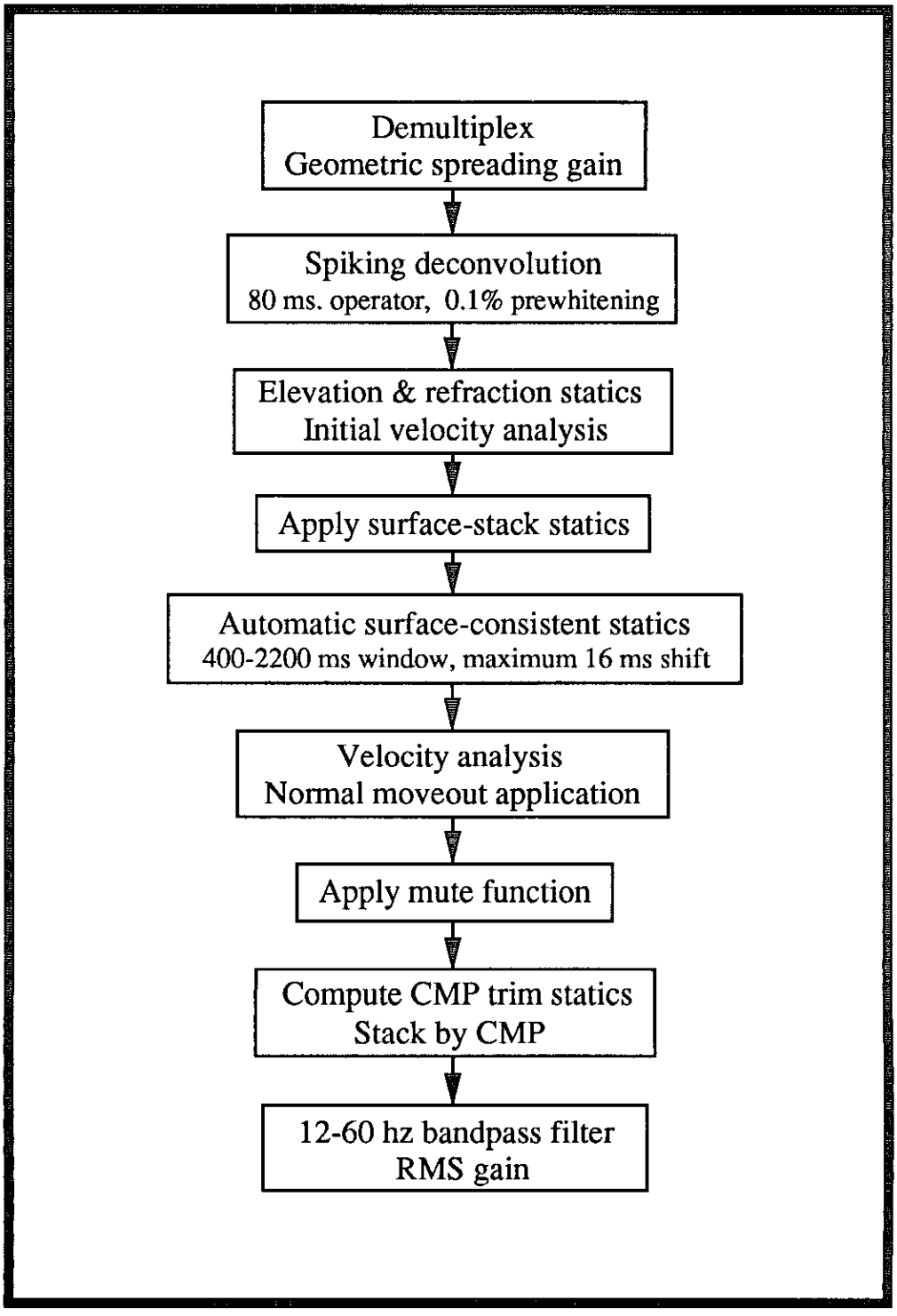

Fig. 6. Processing flowchart for vertical-component (P-P) data.

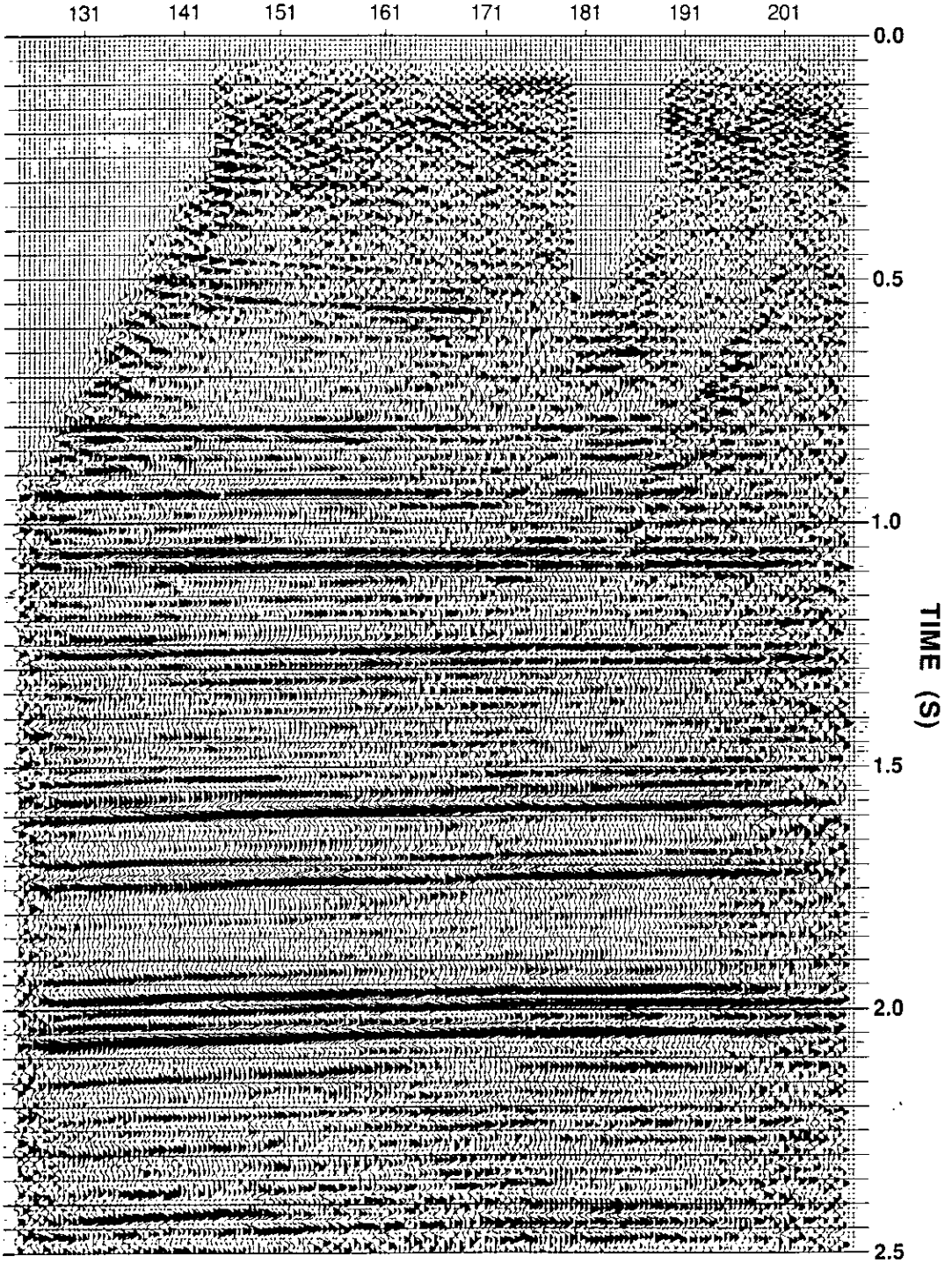

Fig. 7. Stack section of single, vertical-component data.

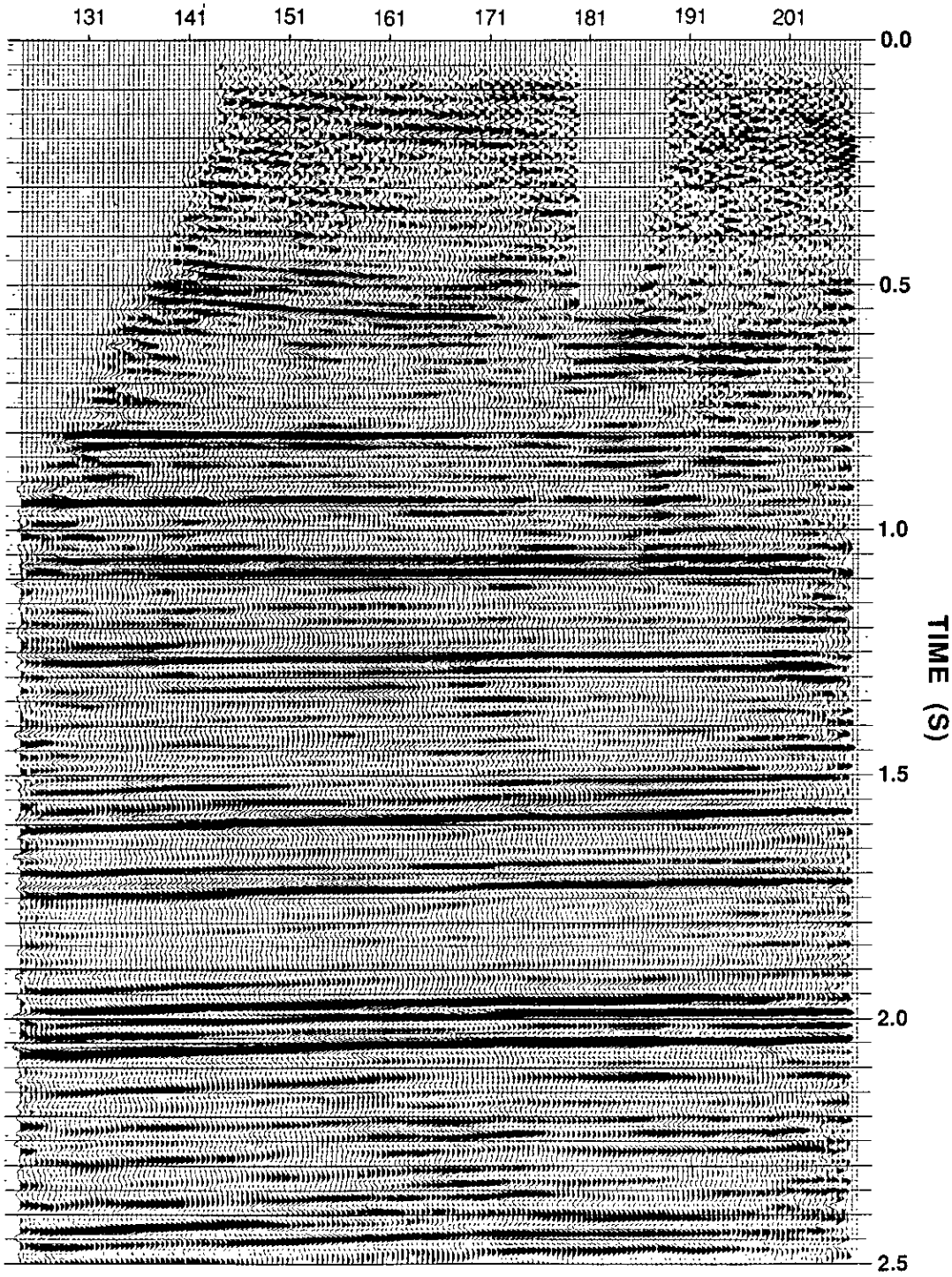

Fig. 8. Stack section of single, vertical-component data with post-stack f-x and f-k filters applied.

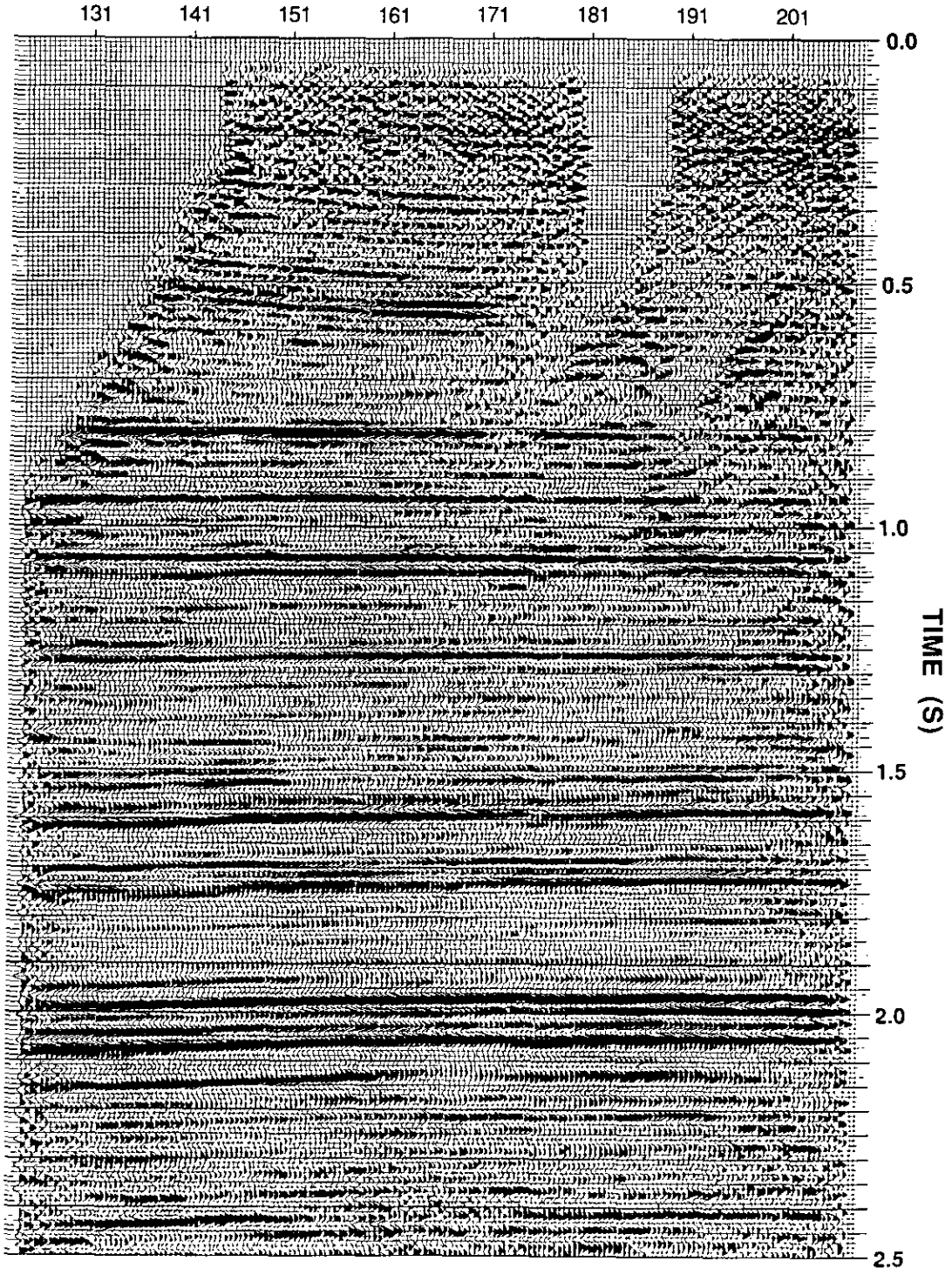

Fig. 9. Stack section of conventional, vertical-component data.

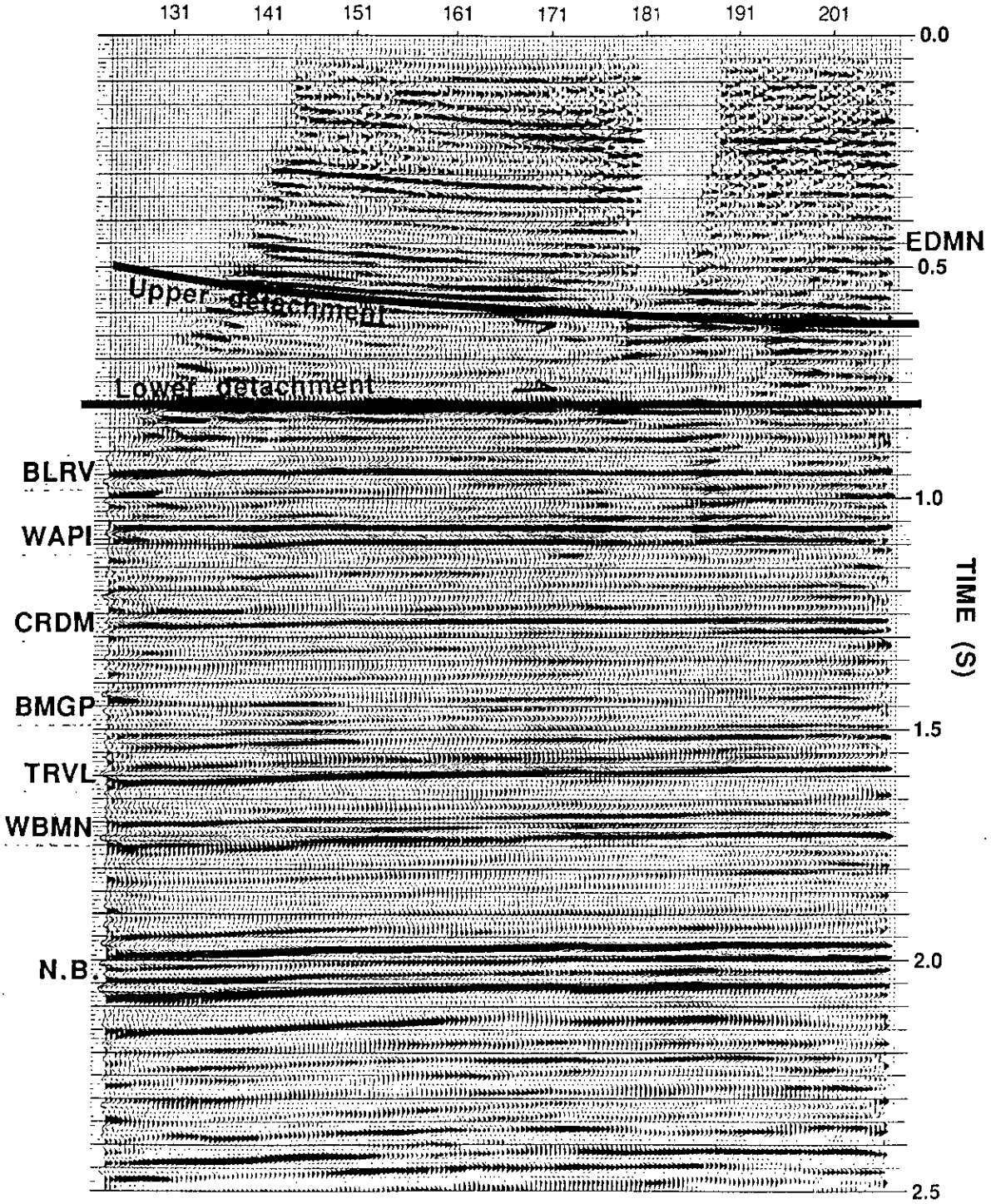

Fig. 10. Stack section of conventional, vertical-component data with post-stack f-x and f-k filters applied.

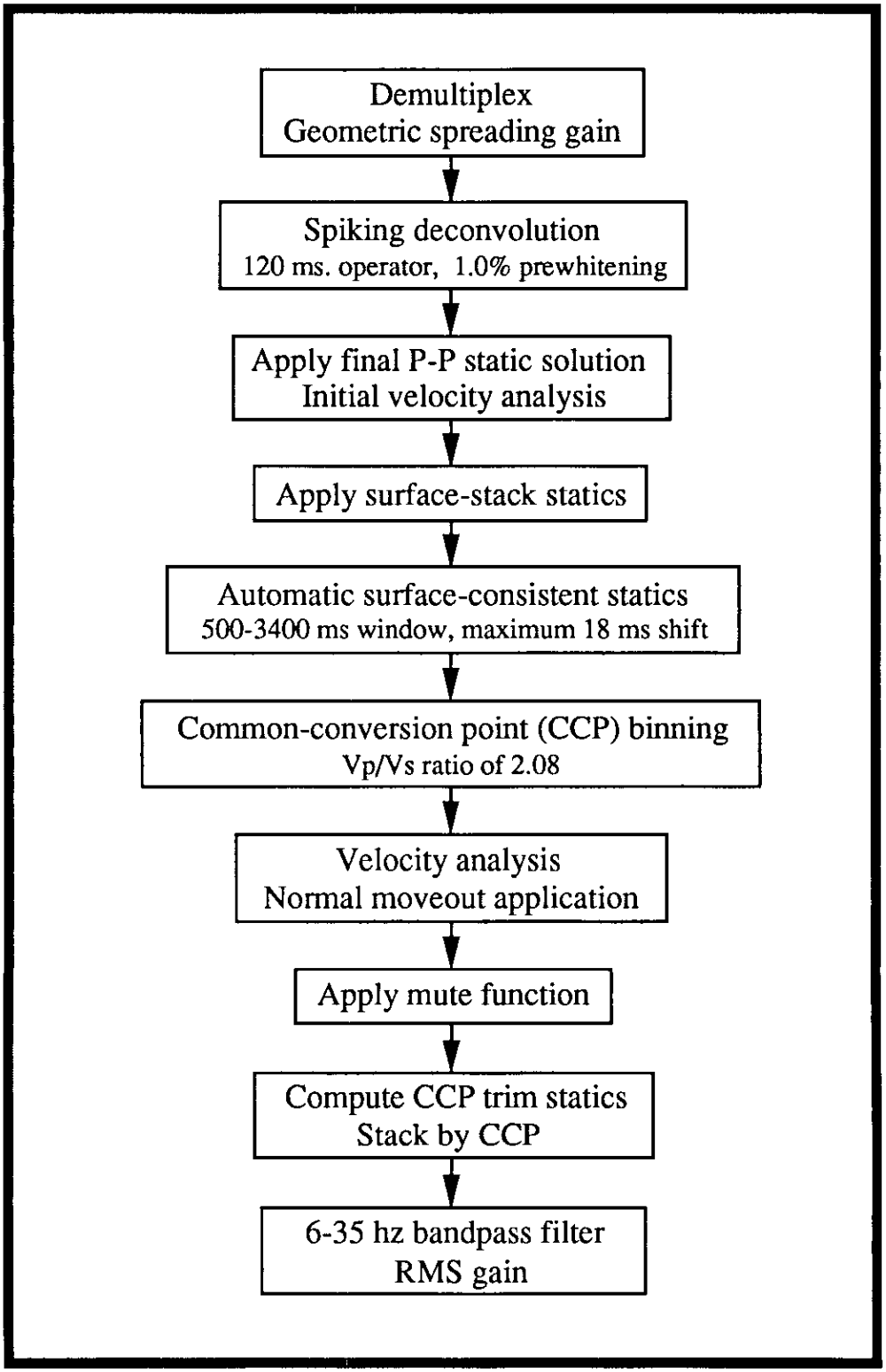

Fig. 11. Processing flowchart for radial-component (P-SV) data.

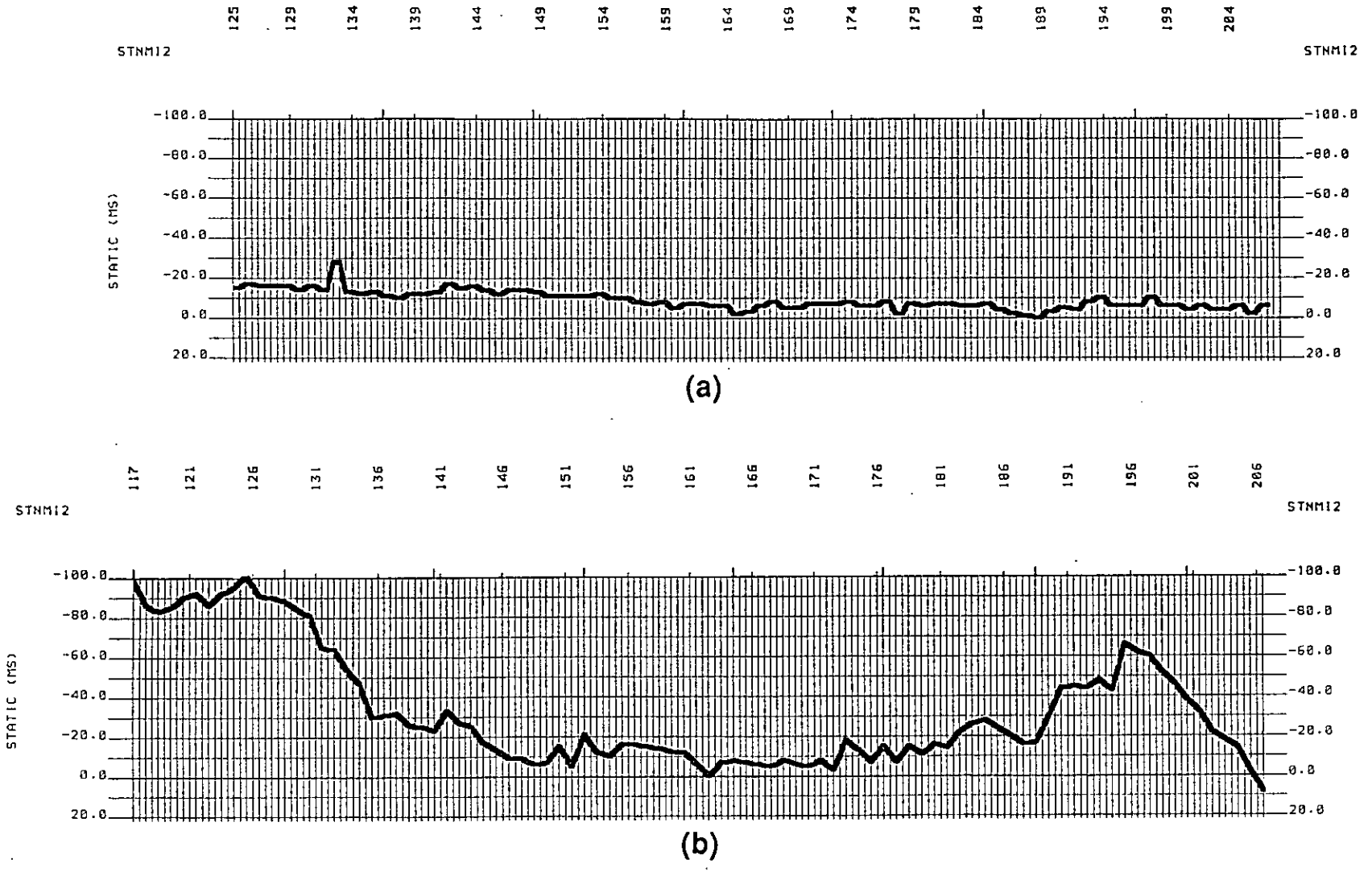

Fig. 12. Final statics solutions for line FS90-1: (a) vertical component (P-P); (b) radial component (P-SV).

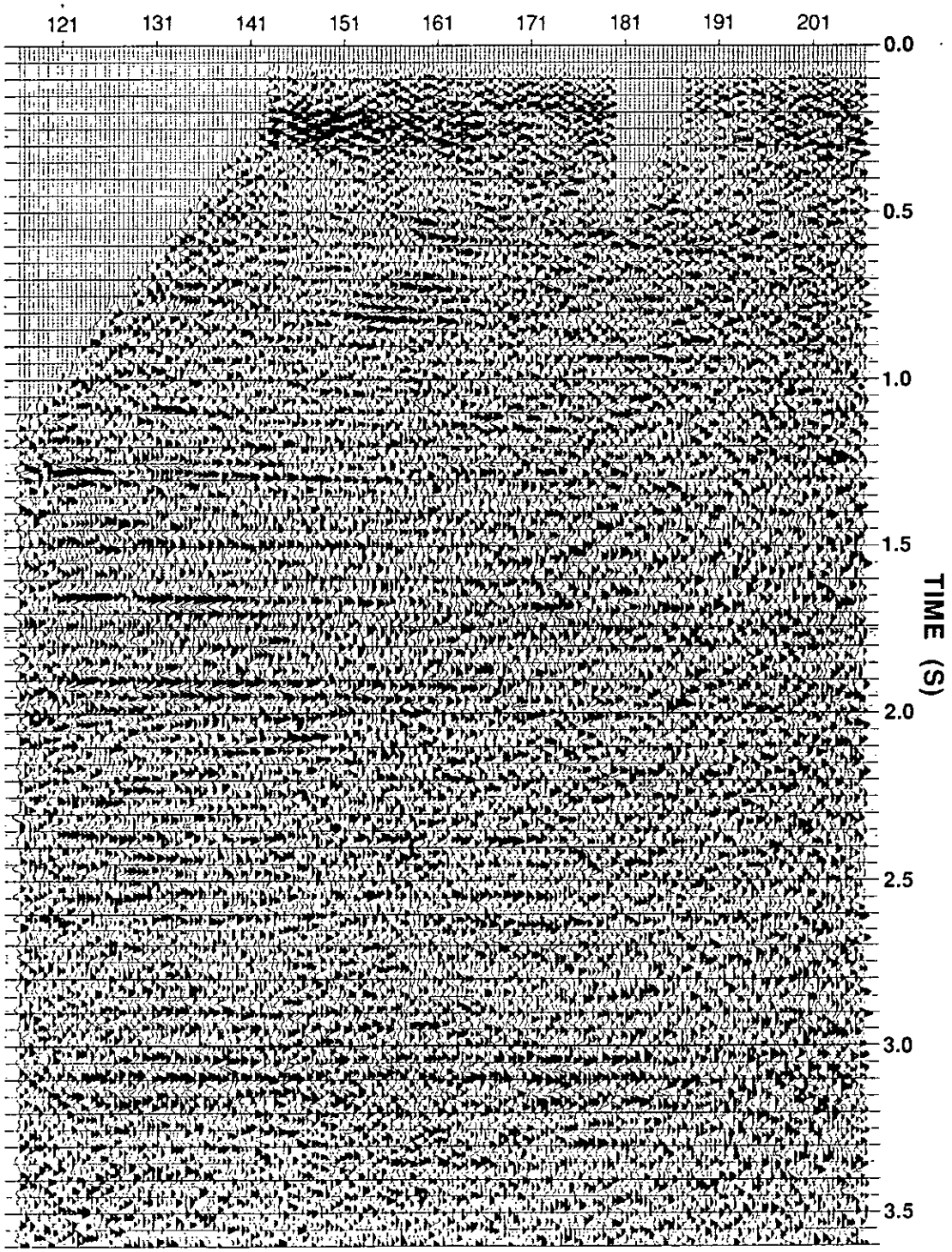

Fig. 13. Stack section of single, radial-component data with asymptotic binning.

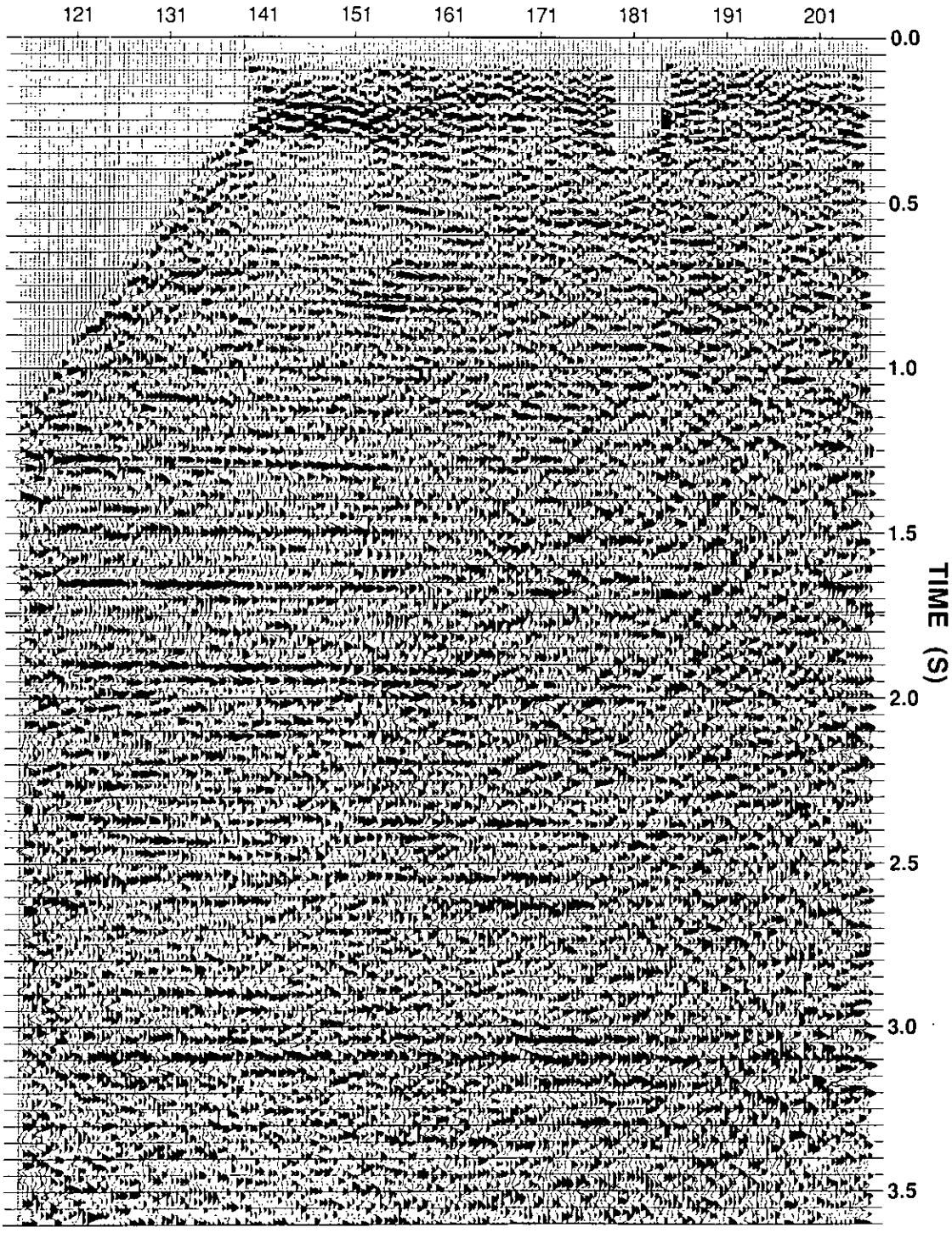

Fig. 14. Stack section of single, radial-component data with depth-variant mapping.

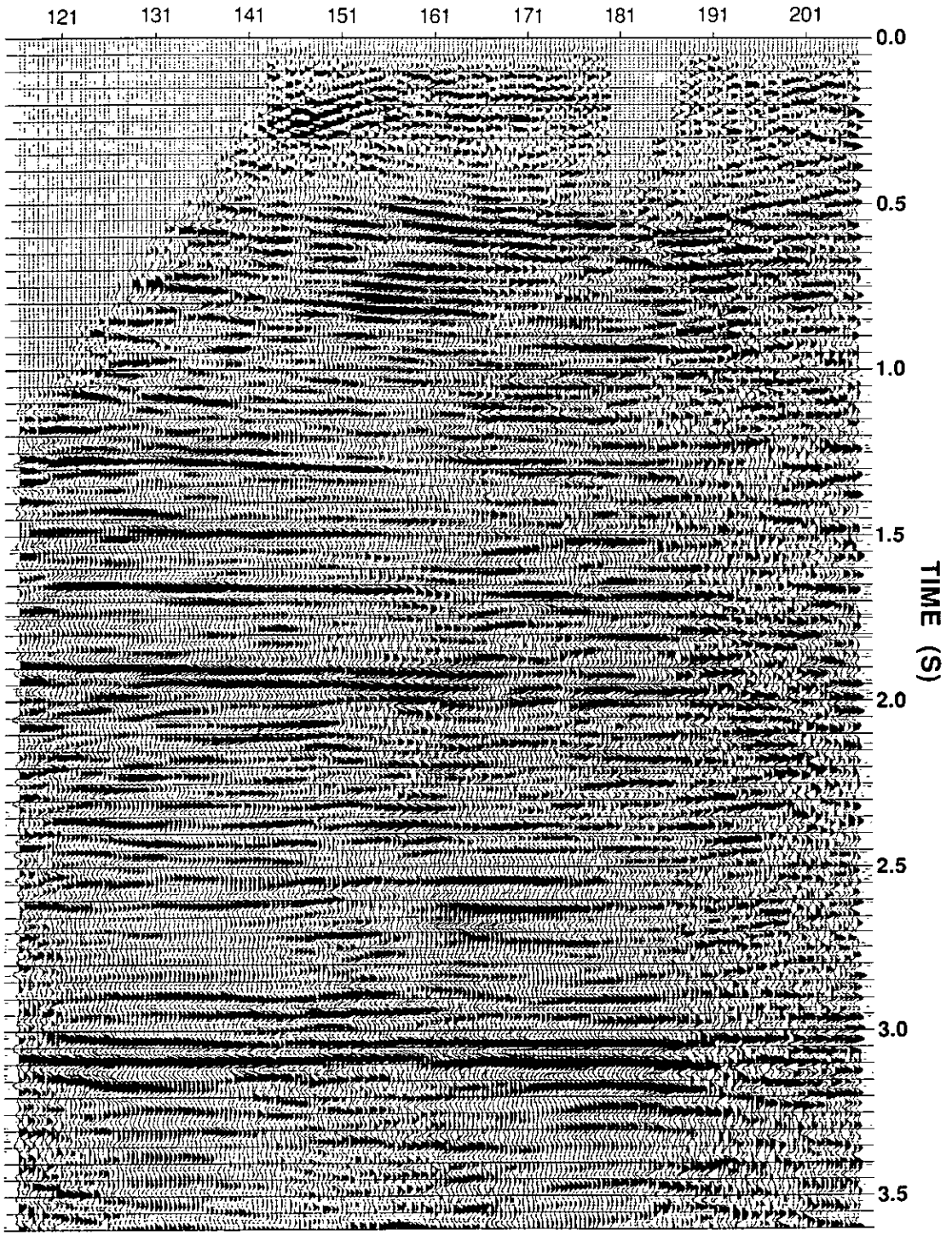

Fig. 15. Stack section of single, radial-component data with asymptotic binning and post-stack f-x and f-k filters applied.

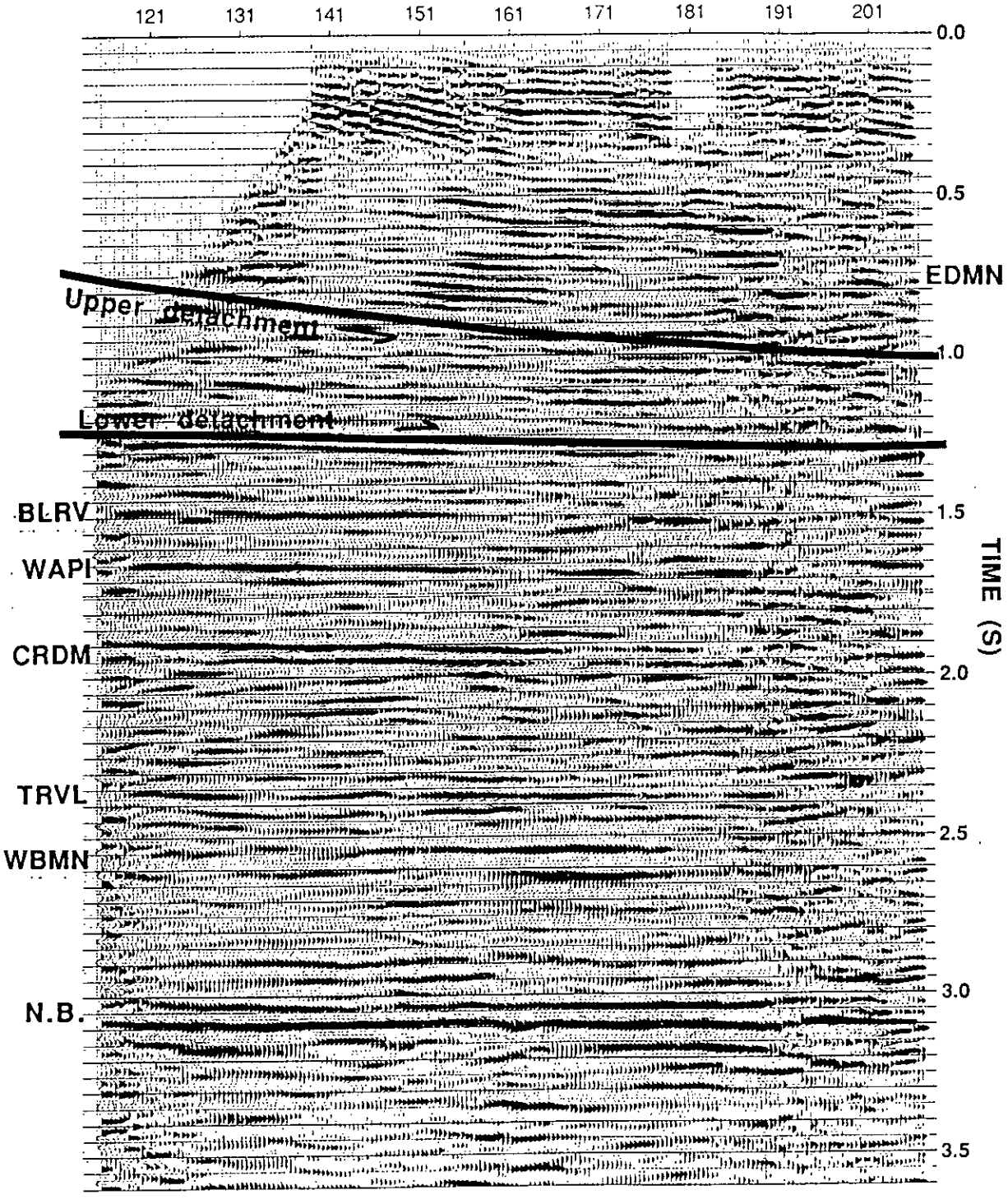

Fig. 16. Stack section of single, radial-component data with depth-variant mapping and post-stack f-x and f-k filters applied.

obtained with point receivers. After the application of post-stack f-x and f-k filters, both sections (Figures 8 and 10) are of comparable quality, although the shallow data are still more coherent in the conventional data (Figure 10).

In comparison, bandpass-filtered sections of the radial-component data (Figures 13 and 14) contain a much higher level of noise than the section from the vertical-component data (Figure 7). The origin of the noise is evident in common-offset stacks for the conventional (P-P), vertical-component (P-P) and radial component (P-SV) data, shown in Figures 17a, 17b and 17c respectively. Figures 17a and 17b are quite comparable, but the radial-component common-offset stack (Figure 17c) shows high-amplitude shot-generated noise which is visible at all offsets and overwhelms reflections at source-receiver offset ranges of up to 600 m. The origin and characteristics of this noise are discussed by Miller et al. (1990).

Figure 14 shows that depth-variant mapping of converted-wave data results in better imaging of shallow reflections than the gathering and stacking of this type of data using an asymptotic appproximation (Figure 13). The signal-to-noise ratio of both the P-SV sections is improved substantially after the application of post-stack f-x and f-k filters (Figures 15 and 16). In these displays, the quality of the data deteriorates at the eastern (right) end of each sections because of the decreasing offset range within each trace gather towards this end of the line.

INTERPRETATION

Geological interpretations of the P-P and P-SV sections are shown in Figures 10 and 16 respectively, with the main geological horizons identified, and the upper and lower detachments of the triangle zone indicated. The shallow part of the section is seen to be much better imaged in the new P-P data than in the older data (Figure 3) and allows the eastern limit of triangle zone deformation to be established. No additional thrust faults are interpreted to be present in the sections.

Most of the major P-P reflections (Figure 10) can be correlated with P-SV reflections (Figure 16), although there are significant differences in relative amplitudes between events. For example, the Mississippian reflection is stronger and more continuous on the P-P section than on the P-SV section, but the converse is true for the Cardium event. These differences can be seen more easily when the sections are juxtaposed (Figure 18) and perhaps could ultimately be interpreted in terms of the petrophysical properties of these formations.

Another interesting aspect of the P-SV sections is that the basement event (3.2 seconds) appears to be one of the most clearly defined reflections, even though the maximum incident angle at this depth is only about 10 degrees.

CONCLUSIONS

This study has shown that reasonable quality P-SV reflection data has been acquired in the Springbank area of Alberta, near the eastern limit of the triangle zone of the Rocky Mountain Foothills. The converted-wave data were acquired in conjunction with production P-P data, and different recording geometries for the two types of surveys are not required. In general, the the amplitude of shot-generated noise on the radial component

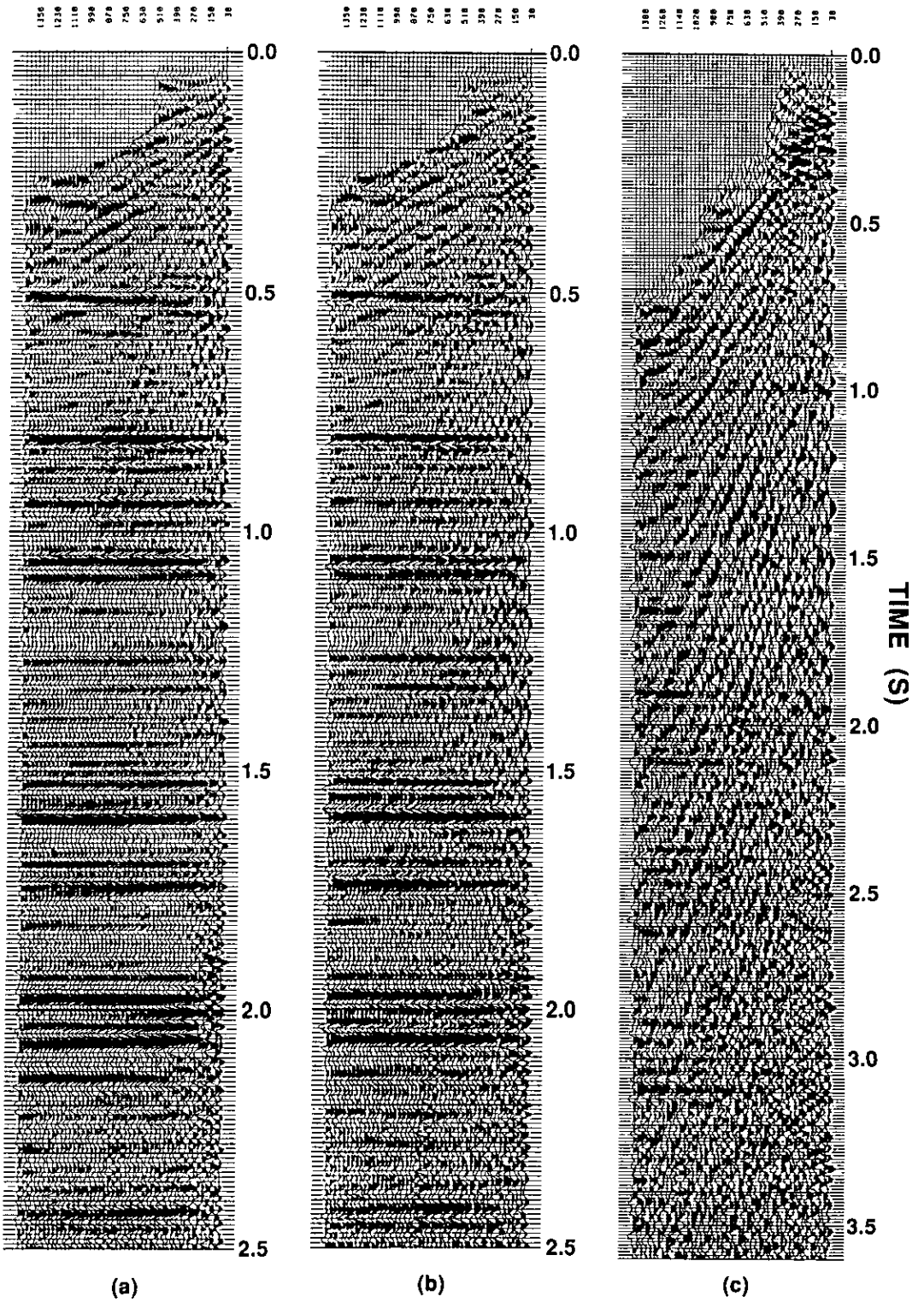

Fig. 17. Common-offset-stack from central part of FS90-1: (a) conventional; (b) vertical component; (c) radial component.

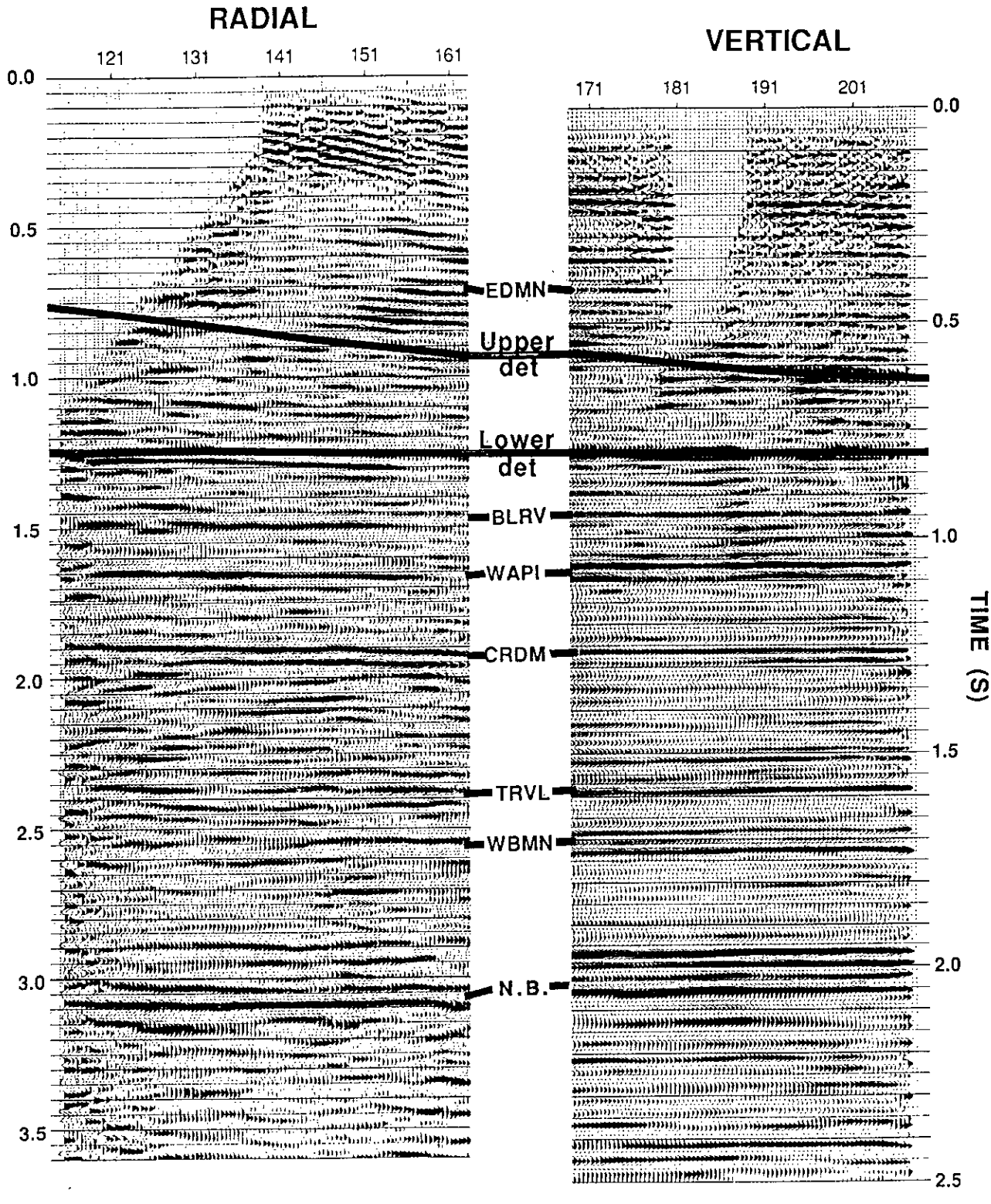

Fig. 18. Spliced vertical and radial-component sections from Figures 10 and 16, showing correlation of main reflections.

is significantly greater than that on the vertical component, and may overwhelm shear-wave reflections over offset distances of up to 600 m from the shot.

Key aspects of processing the converted-wave data were the calculation of shear-wave static corrections from shot and receiver stacks, and the application of post-stack f-x and f-k filters to attenuate random and dipping noise. Final sections of similar quality were obtained from the conventional P-wave survey, which was recorded with a 30 m geophone array, and the vertical-component data, which was recorded with a single receiver at each station. However, the shallowest reflections were better resolved in the former section.

Interpretation of the data showed that reflections from most of the major geological formation boundaries can be identified on both the P-P and P-SV sections, although there are significant differences in relative amplitudes between the two sections. Strong converted-wave reflections from near-basement reflectors were recorded.

ACKNOWLEDGEMENTS

The data were collected by staff and students participating in the 1990 University of Calgary Geophysics Field School, and assisted by Eric Gallant of the CREWES Project. In particular we thank Malcolm Bertram and Carl Gunhold for maintaining the field equipment and offering many helpful suggestions. All data processing was performed using Western Geophysical software operating on the CREWES Project IBM data processing facility.

REFERENCES

Charlesworth, H.A.K., Johnston, S.T., and Gagnon, L.G., 1987, Evolution of the triangle zone in the Rocky Mountain foothills of central Alberta: Can. Journ. Earth Sc., 24, 668-1678.

Eaton, D., and Stewart, R., 1989, Aspects of seismic imaging using P-SV converted waves: CREWES project annual report, v. 1, 68-92.

Fromm, G., Krey, Th. and Wiest, B., 1985, Static and dynamic corrections, in Dohr, G. Ed., Seismic Shear Waves: Handbook of Geophysical Exploration, v. 15a, 191-225.

Garotta, R., Marechal, P., and Magesan, M., 1985, Two-component acquisition as a routine procedure for recording P-waves and converted waves: Jour. Can. Soc. Explor. Geophys., v. 21, 40-53.

Gordy, P.L., Frey, F.R., and Norris, D.K., 1977, Geological guide for the CSPG and the 1977 Waterton Glacier Park Field Conference: C.S.P.G., Calgary, 93 p.

Harrison, M.P., 1989, Three-component seismic data processing: Carrot Creek, Alberta: CREWES project research report, v. 1, 6-26.

Jones, P.B., 1982, Oil and gas beneath east-dipping underthrust faults in the Alberta foothills: in Powers, R.B. (Editor), Geological studies of the Cordilleran thrust belt: Rocky Mountain Association of Geologists Bull, 1, 31-38.

Jones, P.B., 1989, Structural geology of the Alberta Foothills front in the Calgary region, a field guide: International Tectonic Consultants Ltd, Calgary.

McMechan, M.E., 1985, Low-taper triangle-zone geometry: an interpretation for the Rocky Mountain Foothills, Pine Pass - Peace River arc, British Columbia, Bull. Can. Petr. Geol., 33, 31-38.

Miller, S.L., Bertram, M.B., and Lawton, D.C., 1990, Noise analysis if multicomponent seismic data: in this volume.

Price, R.A., 1986, The southeastern Canadian Cordillera: thrust faulting, tectonic wedging, and delamination of the lithosphere: Jour. Struct. Geol., 8, 239-254.

Slotboom, R.T., Lawton, D.C., and Spratt, D.A., 1990, The triangle zone in the Jumping Pound-Wildcat area, Alberta: Abstract, C.S.E.G. Convention, Calgary, May 16, 1990.

Teal, P.R., 1983, The triangle zone at Cabin Creek, Alberta: in Bally, A.W., (Editor), Seismic expression of structural styles: A.A.P.G. Studies in Geology, Series 15, 3, 48-53.